

POLYPHASE ADAPTIVE FILTER BANKS FOR FINGERPRINT IMAGE COMPRESSION

Ömer N. Gerek, A. Enis Çetin

Dept. of Electrical Engineering, Bilkent University,
Bilkent, TR-06533, Ankara, TURKEY

Tel: +90 312 266 4307; fax: +90 312-266 4126

e-mail: gerek@ee.bilkent.edu.tr

ABSTRACT

Subband decomposition is widely used in signal processing applications including image and speech compression. In this paper, we present Perfect Reconstruction (PR) polyphase filter bank structures in which the filters adapt to the changing input conditions. This leads to higher compression results for images containing sharp edges such as fingerprint images. The fingerprint image compression is an important problem due to the high amount of fingerprint images in databases [1]. For example, the FBI database contains 30 million sets of fingerprints. We experimentally observed that our method is successful for binary and gray-valued fingerprint images.

1 PR Adaptive Polyphase Filter Banks

We propose an adaptive subband structure to decompose the fingerprint images. The decomposed images are then quantized using embedded zerotree coding. The adaptive filter banks can be visualized as a polyphase structure in which one of the subband components is predicted from the other subband component. Consider the simple two band PR polyphase decomposition structure shown in Figure 2 in which the filter P_1 can be either linear

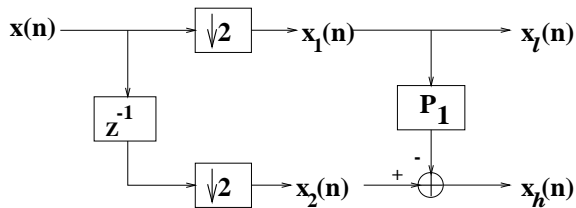


Figure 1: Polyphase analysis structure

or nonlinear [2],[3]. A good P_1 filter would be the one that can predict the samples of $x_2(n)$ as close

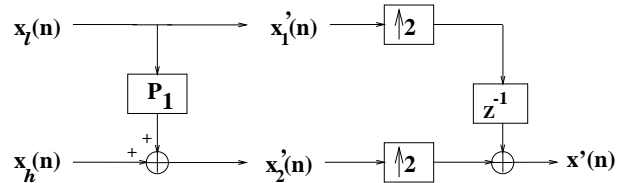


Figure 2: Polyphase synthesis structure

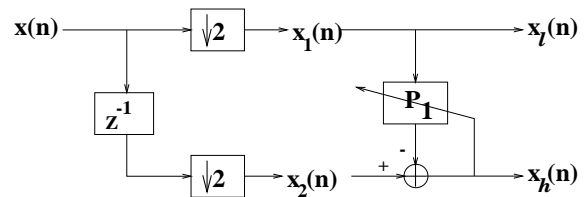


Figure 3: Adaptive structure analysis stage

as possible. This is equivalent to removing the correlated portions of the original signal to achieve high compression. Perfect reconstruction is possible with the structure given in Fig. 2. In this paper, the adaptive FIR filters and adaptive order statistics filters are used in the filter bank and image coding algorithms are developed based on this polyphase structure.

The adaptive filter bank concept is inserted in the prediction stage of the polyphase structure in Fig. 2 and the adaptive polyphase structure is obtained in Fig. 3. In this figure, the signal $x_2(n)$ is again predicted from $x_1(n)$. Furthermore, the pre-

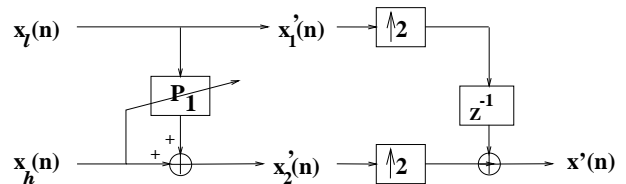


Figure 4: Adaptive structure synthesis stage

diction filter adapts its coefficients, a_k 's, to minimize the variance of $x_2(n)$. In our experiments, we use an LMS-type algorithm [4],[5] is used for updating the equations.

Perfect reconstruction of this decomposition scheme is possible. The parameters $x_1(n)$ and $x_2(n)$ are passed to the decoder. Since $x_2(n)$ corresponds to the error signal in the adaptation algorithm, the decoder can also update the filter coefficients with the same input ($x_1(n)$) and error ($x_2(n)$) sequences as shown in Fig. 4.

The variance of $x_2(n)$ is minimized with the adaptive algorithm. This means that the subband coding gain G_{SBC} is maximized by minimizing $\sigma_{x_2}^2$ because:

$$G_{SBC} = \frac{\sigma_x^2}{(\sigma_{xl}\sigma_{xh})} \quad (1)$$

2 Adaptation Methods

The adaptive estimator for $x_h(n)$ is illustrated in Fig. 3. The FIR adaptive filter is obtained by predicting $x_2(n)$ from $x_1(n)$ in a Linear Minimum Mean Squared Error (LMMS) sense as follows:

$$\hat{x}_2(n) = \sum_{k=-N}^N a_k x_1(n-k) = \sum_{k=-N}^M a_k x_1(n-2k) \quad (2)$$

where the filter coefficients a_k 's are updated using an LMS-type algorithm [4], and the subsignal x_h is given by

$$x_h(n) = x_2(n) - \hat{x}_2(n). \quad (3)$$

In our method, we use the normalized LMS type adaptation schemes for linear FIR filters with the following equations.

$$\hat{\mathbf{w}}(n+1) = \hat{\mathbf{w}}(n) + \mu \frac{\tilde{\mathbf{x}}_{\mathbf{n}} e(n)}{\|\tilde{\mathbf{x}}_{\mathbf{n}}\|^2} \quad (4)$$

where $\hat{\mathbf{w}}(n)$ is the weight vector at time instant n ,

$$\tilde{\mathbf{x}}_{\mathbf{n}} = [x_1(n-N), x_1(n-N+1), \dots, x_1(n+N-1), x_1(n+N)]^T, \quad (5)$$

and

$$e(n) = x_2(n) - \tilde{\mathbf{x}}_{\mathbf{n}}^T(n) \hat{\mathbf{w}}(n). \quad (6)$$

In order to further improve the adaptation performance, the step size parameter μ is also adaptively chosen according to the variance of the input \tilde{x}_1 . Since this data is available both at the encoder and at the decoder side, μ can be updated by the

decoder with the same algorithm, and PR property is preserved. In this case, the filter coefficient update equation becomes

$$\hat{\mathbf{w}}(n+1) = \hat{\mathbf{w}}(n) + \mu(\tilde{\mathbf{x}}_{\mathbf{n}}) \frac{\tilde{\mathbf{x}}_{\mathbf{n}} e(n)}{\|\tilde{\mathbf{x}}_{\mathbf{n}}\|^2} \quad (7)$$

The input elements \tilde{x}_1 and \tilde{x}_2 are selected from a two dimensional region of support which consists of polyphase components of an image matrix in horizontal and vertical directions.

Another choice for P_1 is the adaptive Order Statistics (OS) filter [7]-[10]. Similar to the adaptive FIR case, the OS filters can be adapted by minimizing the subsignal y_2 using an adaptation strategy. The rank ordering of the input elements gives better coding results especially for the images that contain regions separated by edges. At the edges, the median characteristics of the adaptive OS filter eliminates the ringing effects. In our simulations, we used a region of support with 9 elements. After rank ordering these elements, the largest and the smallest values are ignored, and the remaining rank ordered elements are fed to an LMS adaptation block.

3 Compression of Gray Tone and Binary Fingerprint Images

The compression of gray tone fingerprint images is performed by applying the adaptive subband decomposition followed by an Embedded ZeroTree (EZT) coder [11]. The level of decomposition is determined by the size of the image. The OS adaptive filters gave slightly better results than the FIR adaptive filters for the fingerprint images. Five level decomposition is used for 256×256 images. Experimental results show that our decomposition scheme with the EZT coder outperforms the traditional Embedded Zerotree Wavelet (EZW) coder [11] in which a fixed wavelet decomposition is performed first, and the coefficients are compressed by the EZT method.

The compression of binary fingerprint images need more elaboration. The straight application of the adaptive subband decomposition followed by the EZT coder increases the dynamic range of the reconstructed image. To avoid this increase in the range, a modified decomposition and quantization scheme to keep the decoded signal in the binary range is developed.

The LMS algorithm usually produces non-integer coefficients, so the filtered signal is not integer in general. Furthermore, for the black regions of a fingerprint image where most of the pixel values are zero, the LMS filter becomes unstable. As a result, the LMS algorithm is disabled in the regions where the majority of the pixels are either black or white, and the prediction value is set to the majority of the pixel values. In the flat regions (black or white) of a fingerprint image, the high band sub-signal becomes zero. The prediction errors occur in the transition regions which correspond to the edge portions of the fingerprint image. Therefore, high pass signal $x_h(n)$ contains non-zero elements only in transition regions. This shows that the low and high band signals are completely decorrelated by the adaptive subband decomposition scheme. It is observed that the quantization of these subband signals does not produce ringing effects in the decoded image. The only visible effect in the reconstructed image is an occasional shift in the edge region which separates the black and white regions. In our simulation studies, the subband signals of the binary fingerprint image are quantized by an EZT type coder.

In the decoder side, the filter bank switches between the adaptive and fixed prediction filter banks depending on the number of black or white pixels in the region of support in $\tilde{\mathbf{x}}_n$. Finally, the reconstructed image is quantized to binary with a threshold.

4 Simulation Studies

In our simulation studies, we used 20 fingerprint images taken from the National Institute of Standards and Technology (NIST) database examples for compression. All of the fingerprint images used are 8 bit 256x256 images. For the binary image simulation studies, we quantized these images to binary with an appropriate threshold level. Examples of these images are shown in Fig. 5.

In Fig. 6, the coded versions of a gray-tone fingerprint image are shown. Our nonlinear adaptive algorithm accomplished a compression ratio of 15.5:1 at PSNR = 30dB whereas the well known EZW coder [11] had a compression ratio of 13.0:1 at the same PSNR value. Furthermore, the ringing effects present in the EZW coded image are eliminated with the use of our method.

In Fig. 7, the binary fingerprint test image is

compressed to two different compression ratios. The image at the left shows the coded image at 0.057 bpp and the one at the right shows the coded image at 0.072 bpp. Both of the images preserve the discriminating features of fingerprint images such as core and delta points. Our adaptive coding algorithm preserves the visual quality of the original fingerprint images. The JBIG standard could compress the same image only to 0.17 bpp.



Figure 5: Two fingerprint images. Left: binary, right: gray tone



Figure 6: Reconstructed images at CR=18:1(left) and CR=15.5:1 (right).

We also compared the average, minimum, and maximum compression ratios obtained by the adaptive FIR and OS LMS algorithms to the results obtained by an EZW coder for 20 gray tone fingerprint images. The results are presented in Table 1.



Figure 7: Reconstructed images at 0.057 bit/pixel (left) and 0.072 bit/pixel (right).

	Max CR	Min CR	Ave CR
EZW	14.7	12.7	13.2
OS adapt.	15.8	15.0	15.4
FIR adapt.	15.4	14.7	15.0

Table 1: *Experimental results for 20 gray scale fingerprint images at PSNR = 30dB*

	Max CR	Min CR	Ave CR
Adapt.	15.5	12.2	13.8
JBIG	7.9	5.2	6.0

Table 2: *Experimental results for 20 binary fingerprint images at visually transparent quality.*

We observed that the OS adaptation produces the best compression results.

The coding results for the binary images are presented in Table 2 and compared with the JBIG standard. Significant improvements are obtained with the use of the adaptive filter bank.

References

- [1] Federal Bureau of Investigation, "WSQ gray-scale fingerprint image compression specification," document IAFIS-IC-0110v2, Feb. 1993.
- [2] F. J. Hampson and J. C. Pesquet, "A nonlinear subband decomposition with perfect reconstruction," *IEEE Int. Symp. on Image Proc.* 1996.
- [3] Ömer N. Gerek, Metin Nafi Gürcan, A. Enis Çetin, "Binary Morphological Subband Decomposition For Image Coding," *IEEE Int. Symp. on Time-Frequency and Time Scale Analysis*, 1996.
- [4] O. Arıkan, A. E. Çetin, Engin Erzin, 'Adaptive Filtering for non-Gaussian stable processes,' *IEEE Signal Processing Letters*, vol. 1, No. 11, pp. 163-165, November 1994.
- [5] Gül Aydın, O. Tanrikulu, A. Enis Çetin, "Robust least mean mixed norm adaptive filtering algorithms for α -stable random processes," *IEEE- ISCAS'97*, Hong Kong, June 1997.
- [6] S-M. Phoong, C. W. Kim, P.P Vaidyanathan, R. Ansari, "A new class of two channel biorthogonal filter banks and wavelet bases," *IEEE Trans. Signal Proc.*, Vol.43, No.3, pp. 649-665, March 1995.
- [7] Gonzalo. R. Arce and M. Tian, "Order-statistic filter banks," *IEEE Transactions on Image Processing*, 5, June 1996.
- [8] I. Pitas and A. Venetsanopoulos, "Adaptive filters based on order statistics," *IEEE Trans. Signal Processing*, vol. 39, Feb. 1991.
- [9] P. Salembier, "Adaptive rank order based filters," *EURASIP Signal Processing*, 27(1):1-25, April 1992.
- [10] P. Salembier and L. Jaquenoud, "Adaptive morphological multiresolution decomposition," *In Dougherty Gader, editor, Image Algebra and Mathematical Morphology*, volume 1568, pages 26-37, San Diego, USA, July 1991.
- [11] J. M. Shapiro, "Embedded Image Coding Using Zerotrees of Wavelet Coefficients," *IEEE Trans. on Signal Processing*, vol. 41, no. 12, pp. 3445 - 3462, Dec. 1993.